Cell Reports, Volume *32*

Supplemental Information

In Vivo Estimates of Liver Metabolic Flux Assessed by ^{13}C-Propionate and ^{13}C-Lactate Are Impacted by Tracer Recycling and Equilibrium Assumptions

Clinton M. Hasenour, Mohsin Rahim, and Jamey D. Young

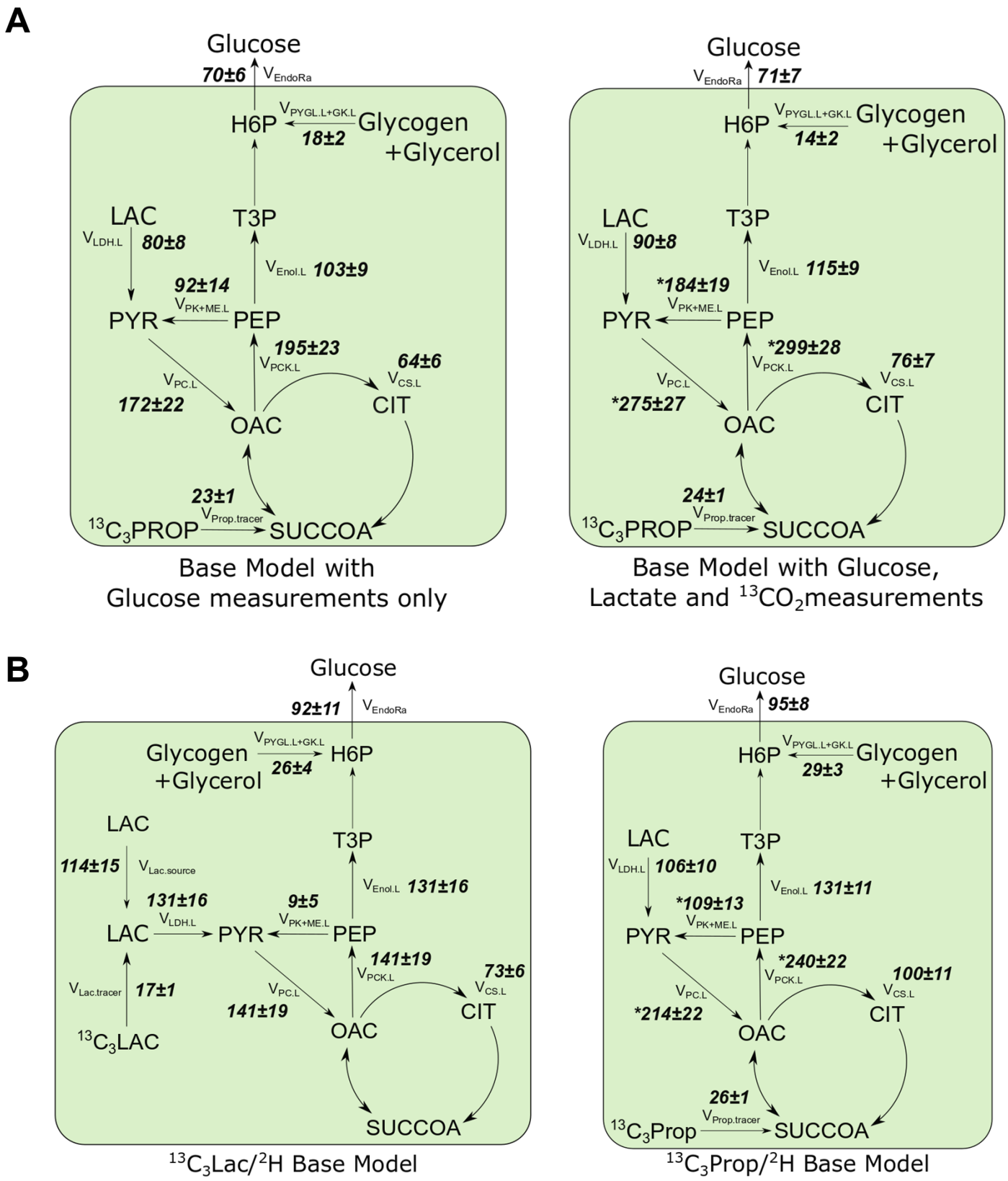

Figure S1. Regression of base model to specific measurement sets. Related to Figures 2, S2, and Table S1

(A) Flux estimates obtained from the base model using plasma glucose MIDs alone contrasted with those that included $^{13}CO_2$ and plasma lactate measurements in the flux regression. Data are presented as means (μmol/kg/min) ± SEM, (n=4) *p<0.05 vs. base model with glucose measurements only

(B) Base model flux estimates from mice infused with $^{13}C_3$Lac/^{2}H or $^{13}C_3$Prop/^{2}H isotopes. Data are presented as means (μmol/kg/min) ± SEM (n=6-7) *p<0.05 vs. $^{13}C_3$Lac/^{2}H base model

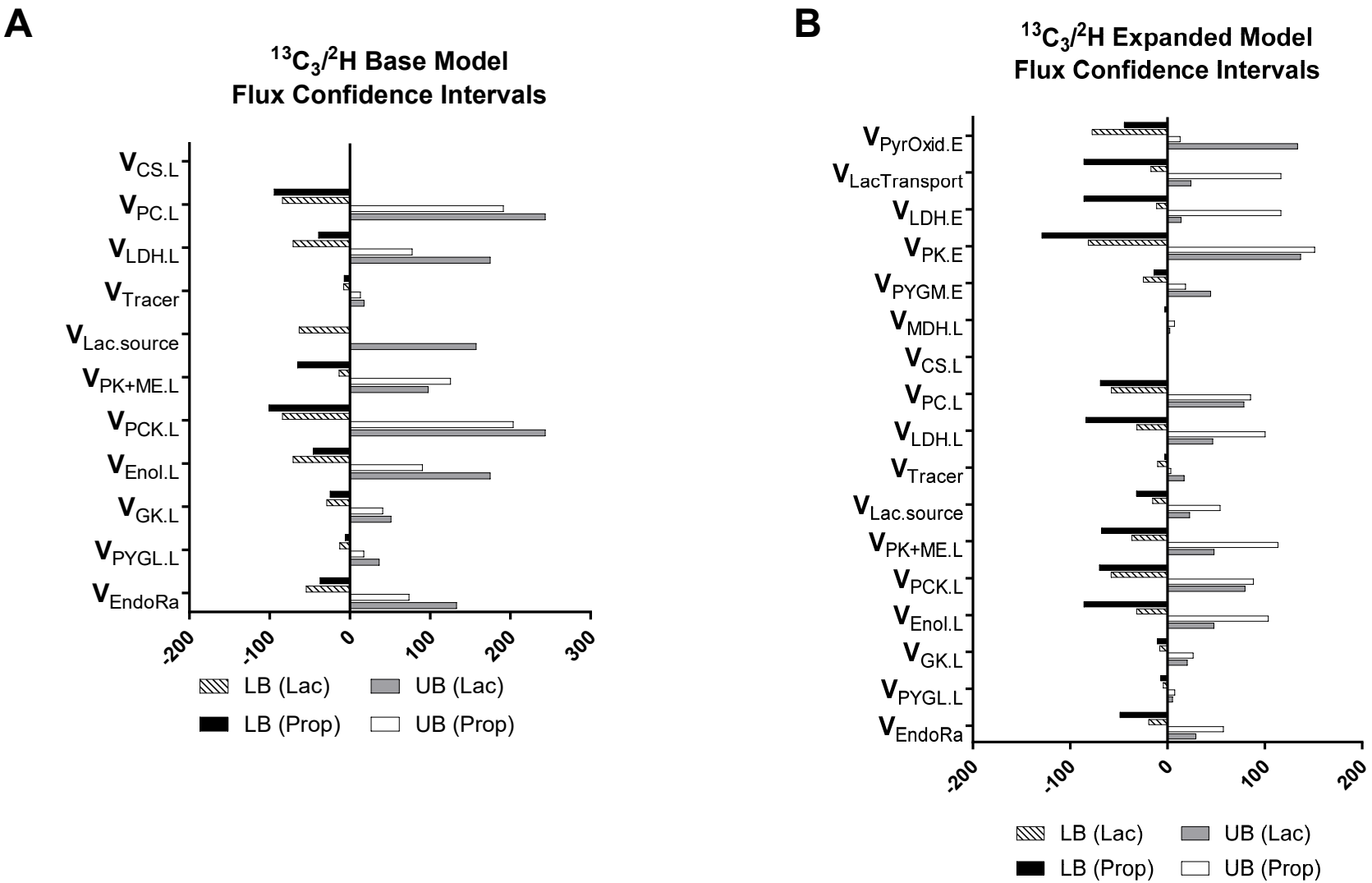

Figure S2. Confidence interval widths in dual tracer models. Related to Figures 2 and 5

95% confidence intervals were calculated for relative hepatic and extrahepatic fluxes in INCA.

(A) $^{13}C_3$Lac/^{2}H (SSR Ave: 19.9±3.5, Expected Range: 11-36.8 DOF: 22) and $^{13}C_3$Prop/^{2}H Base Models (SSR Ave: 32.5±5.4, Expected Range: 11-36.8 DOF: 22). V_{Tracer} represents the flux $V_{Lac.tracer}$ or $V_{Prop.tracer}$ in the liver compartment, depending on the experiment

(B) $^{13}C_3$Lac/^{2}H (SSR Ave: 78.4±8.3, Expected Range: 49.6-96.2, DOF: 72) and $^{13}C_3$Prop/^{2}H Expanded Models (SSR Ave: 70.9±8.1, Expected Range: 49.6-96.2, DOF: 72). V_{Tracer} represents the flux $V_{Lac.inf}$ in blood plasma or the flux of $V_{Prop.inf}$ in the liver compartment, depending on the experiment

Upper and lower bounds are presented as the mean differences (x-axis) from the relative flux estimates (n=5-7). Ranges are expressed relative to $V_{CS.L}$=100. The Expected Range of the SSR is calculated from the 95% confidence limits of a chi-square cumulative distribution function with the indicated degrees of freedom (DOF)

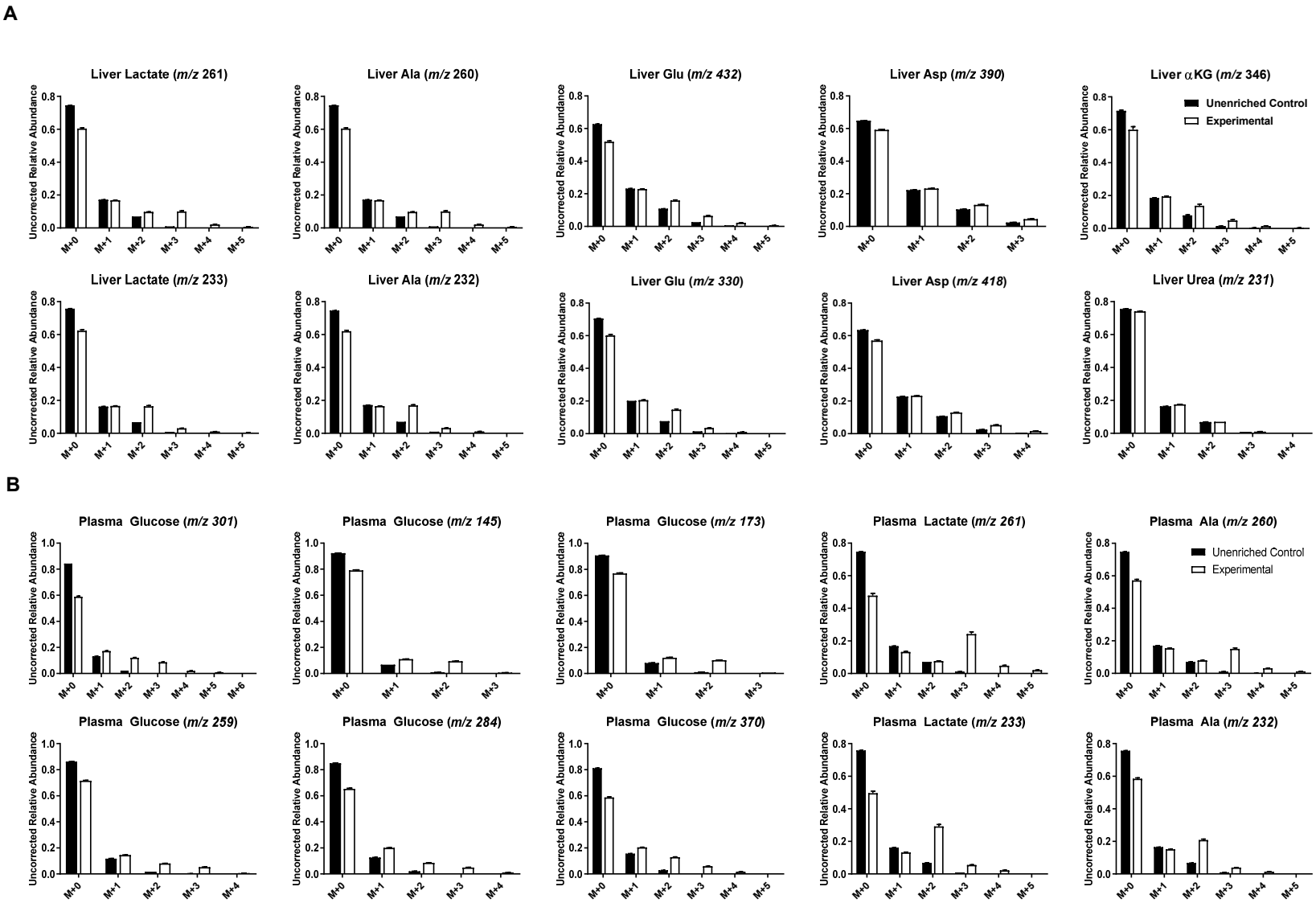

Figure S3. Mass isotopomer measurements for plasma and liver metabolites. Related to Figures 3, 4, S4, S5, S6, and Tables S3 and S5.

(A) Liver lactate (*m/z* 261, 233), alanine (*m/z* 260, 232), glutamate (*m/z* 432, 330), aspartate (*m/z* 418, 390), α-ketoglutarate (*m/z* 346), and urea (*m/z* 231) derivative measurements

(B) Plasma glucose (*m/z* 301,145,173, 259, 284, 370), alanine, (*m/z* 260, 232) and lactate (*m/z* 261, 233) derivative measurements

Enriched mass isotopomer distributions were determined using GC-MS for metabolites extracted from liver and plasma harvested at the close of the experimental period from 19-20hr fasted C57Bl/6J mice infused with $^{13}C_3$Lac. Unenriched samples were obtained from control C57Bl/6 mice for metabolite identification and measurement error determination. Data are presented as means ± SEM (n=7)

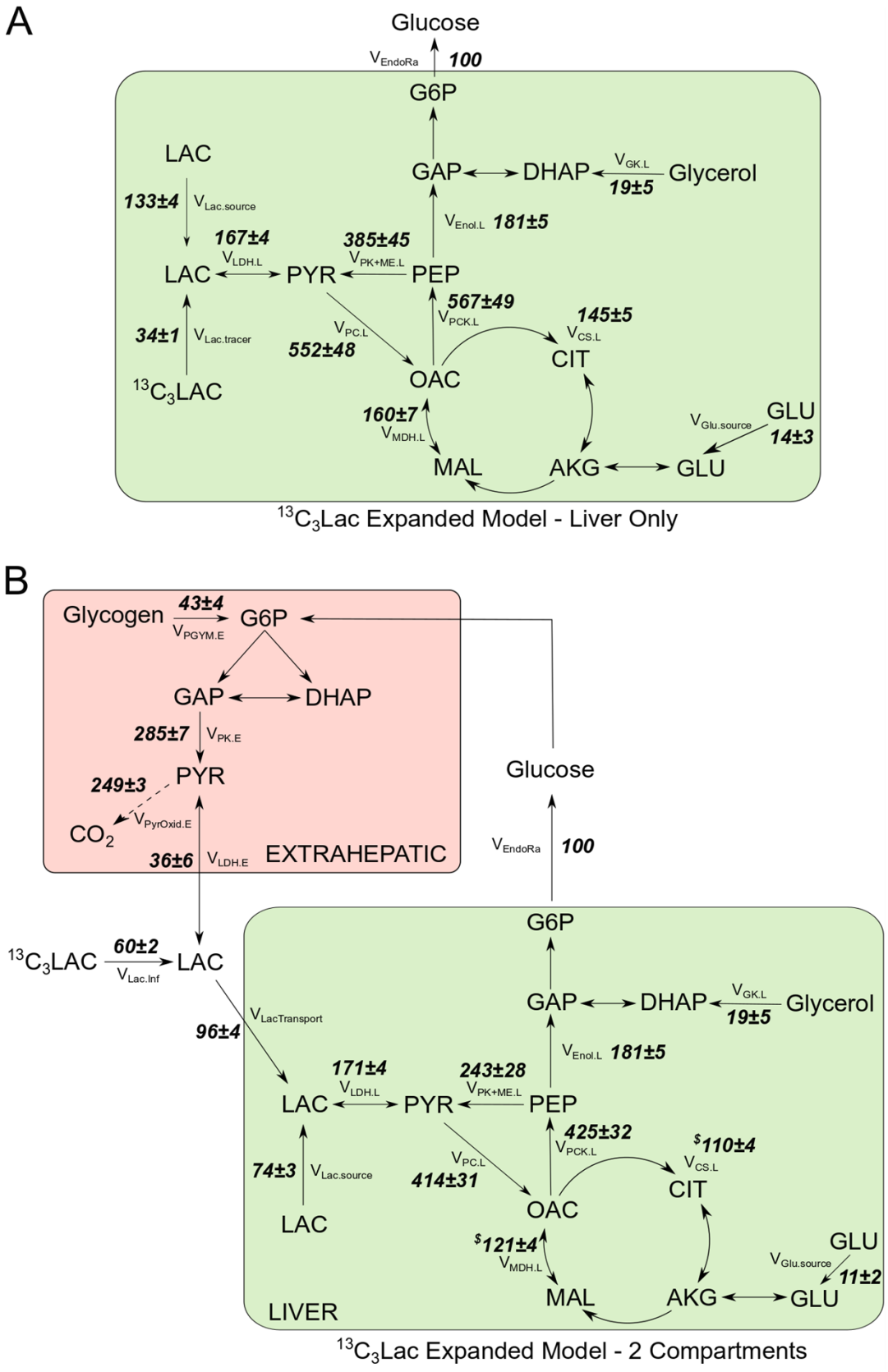

Figure S4. Expansion of models in mice infused with $^{13}C_3$Lac. Related to Figures 4, S3, S5 and Tables S3 and S5

(A) Relative flux estimates from expanded model (liver only) using plasma and liver tissue measurements

(B) Relative flux estimates from the same mice presented in (A) regressed using an expanded model including an extrahepatic compartment to facilitate descriptions of Cori cycling; mice were infused with $^{13}C_3$Lac only.

Data are presented as means ± SEM (n=7) *p<0.05 vs. $^{13}C_3$Lac expanded model – liver only

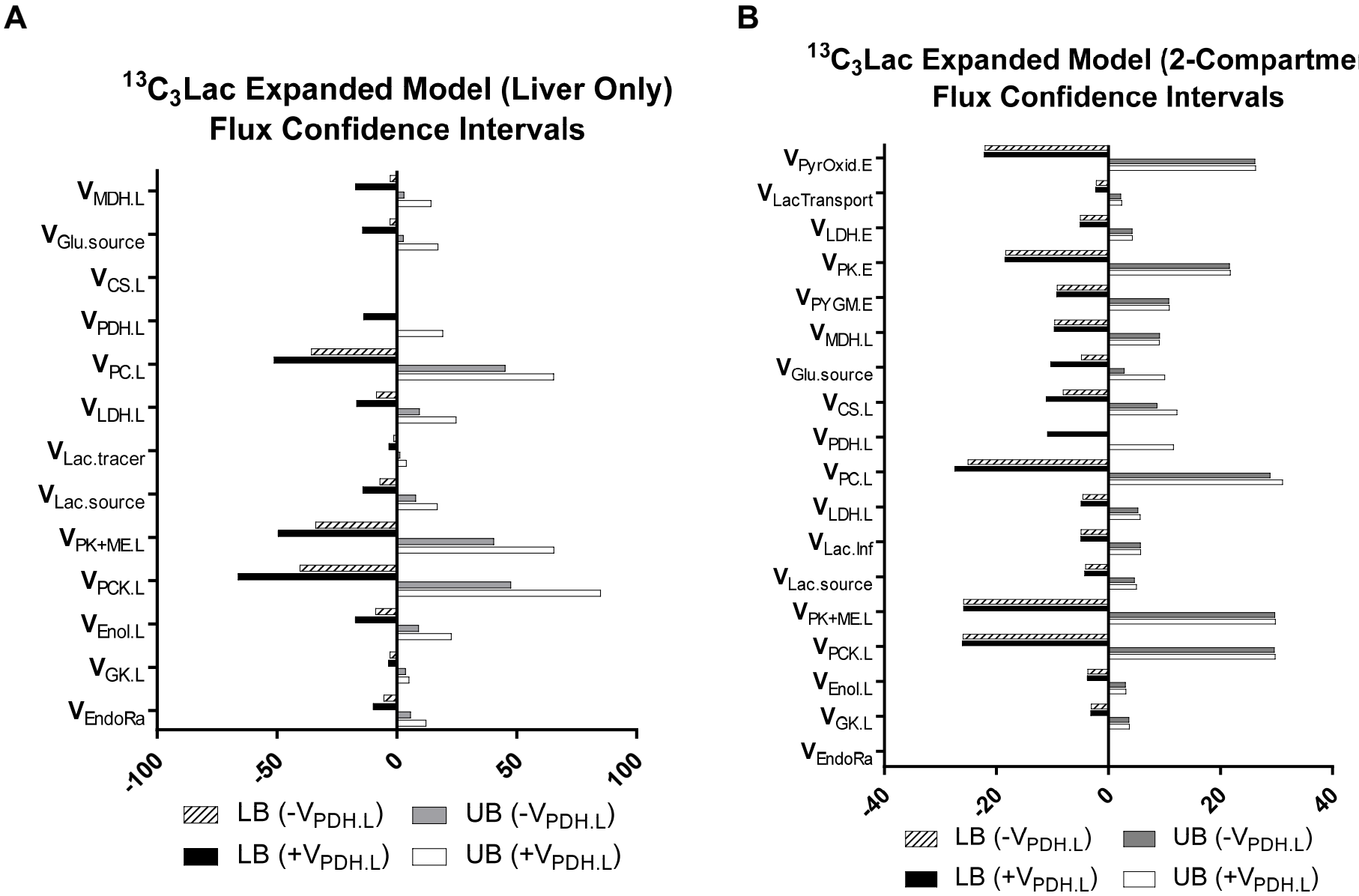

Figure S5. Confidence interval widths in $^{13}C_3$Lac studies. Related to Figures 4, S4 and S6

(A) $^{13}C_3$Lac expanded model – Liver Only for networks without PDH (SSR Ave: 65.1±8.9, Expected Range: 44.6-89.2, DOF: 65) or with PDH (+$V_{PDH.L}$) (SSR Ave: 53.9±6.0, Expected Range 43.8-88, DOF: 64)

(B) $^{13}C_3$Lac expanded model with two compartments for networks without PDH (SSR Ave: 80.7±9.6, Expected Range: 63.1-114.7, DOF: 87) or with PDH (+$V_{PDH.L}$) (SSR Ave: 68.4±6.6, Expected Range: 62.2-113.5, DOF: 86)

Upper and lower bounds are presented as the mean differences (x-axis) from relative flux estimates (n=5-7). Ranges are expressed relative to $V_{CS.L}$=100. The Expected Range of the SSR is calculated from the 95% confidence limits of a chi-square cumulative distribution function with the indicated degrees of freedom (DOF)

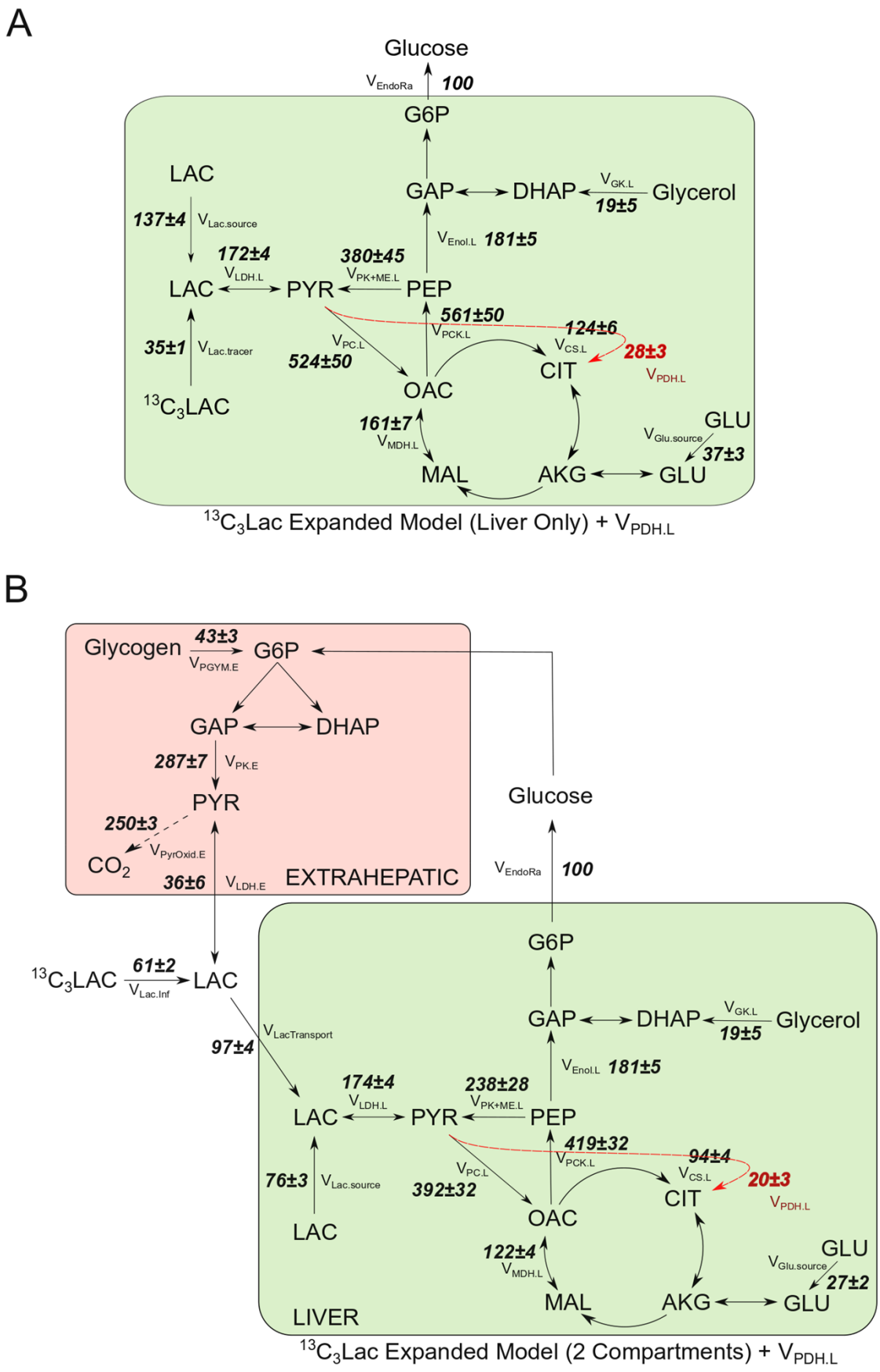

Figure S6. Testing the assumption of low $V_{PDH.L}$ flux during fasting with $^{13}C_3$Lac. Related to Figure 4B, S3, S5, and Tables S3 and S5

(A) Relative flux estimates from expanded model (liver only) using plasma and liver tissue measurements and an active pyruvate dehydrogenase complex (+$V_{PDH.L}$) in the liver

(B) Relative flux estimates from the same mice presented in (A) using a two-compartment expanded model with an active pyruvate dehydrogenase complex (+$V_{PDH.L}$) in the liver

Data are presented as means ± SEM (n=7)

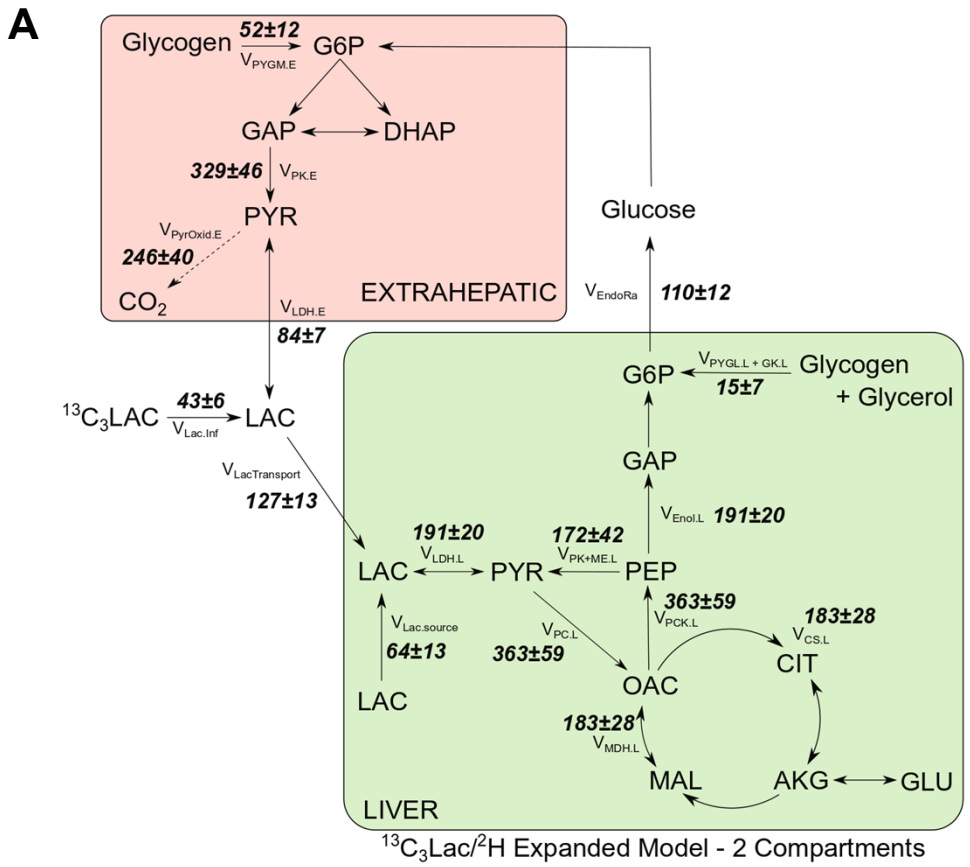

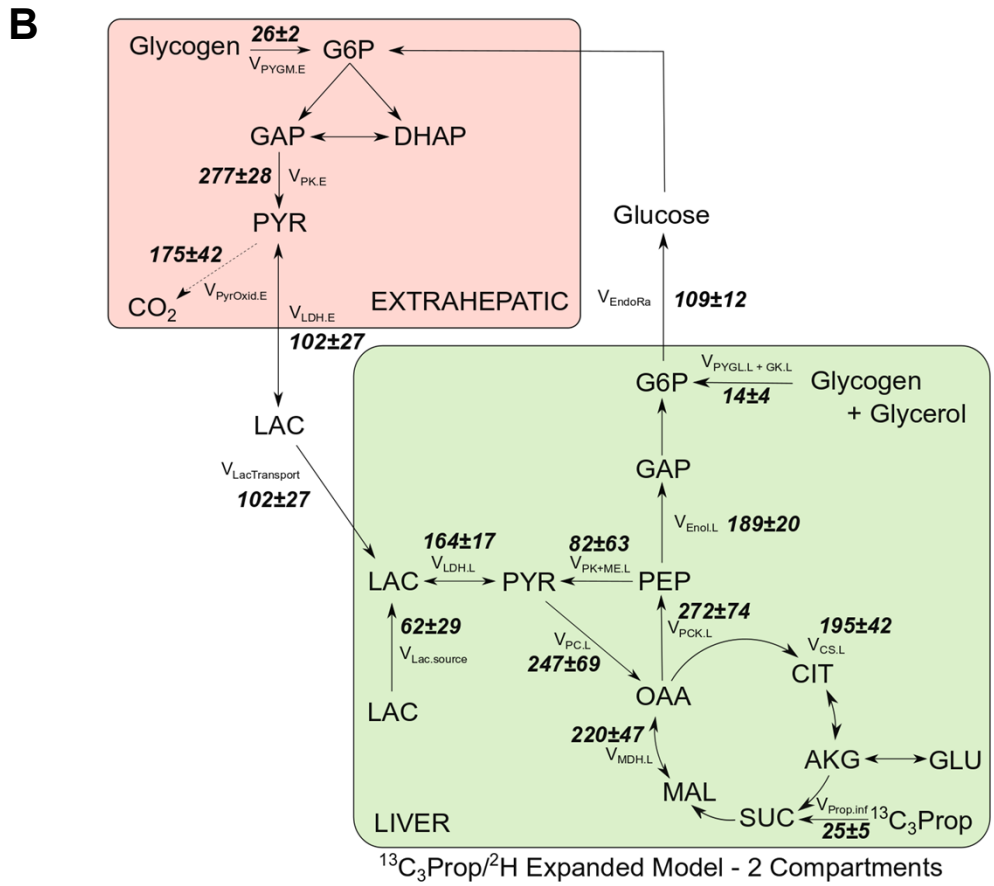

Figure S7. Comparison of $^{13}C_3$Lac/^{2}H and $^{13}C_3$Prop/^{2}H isotopes for hepatic flux estimates using expanded models of metabolism. Related to Figures 5, S2, and Tables S2 and S4

(A) Expanded model (two compartments) showing absolute flux estimates in 19-20hr fasted, C57Bl/6J mice infused with $^{13}C_3$Lac/^{2}H or

(B) $^{13}C_3$Prop/^{2}H isotopes

Data are presented as means ± SEM (µmol/kg/min, n=5)

Flux	Base Model Reaction Network
	Liver Compartment: Glucose Synthesizing and Oxidative Metabolic Reactions
$V_{Glc.inf}$	Glucose.inf (AaBbCcDdEeFfg) → Glucose.P (AaBbCcDdEeFfg)
V_{EndoRa}	H6P (AaBbCcDdEeFfg) → Glucose.P (AaBbCcDdEeFfg)
$V_{PYGL.L}$	Glycogen (AaBbCcDdEeFfg) + H (h) → H6P (AaBhCcDdEeFfg) + H (b)
$V_{Aldo.L}$	T3P (ChBcAab) + T3P (DdEeFfg) + H (i) → H6P (AbBiCcDdEeFfg) + H (h) + H (a)
$V_{GAPDH.L}$	BPG (ABbCcd) + H (e) + H (f) → T3P (AfBeCcd) + H (b)
$V_{GK.L}$	Glycerol (AaeBbCcd) + H (f) → T3P (AeBfCcd) + H (a) + H (b)
$V_{Enol.L}$	PEP (ABCcd) + H (b) → BPG (ABbCcd)
$V_{PK+ME.L}$	PEP (ABCab) + H (c) → Pyr (ABCabc)
$V_{LDH.L}$	Lac (ABbCcde) → Pyr (ABCcde) + H (b)
$V_{Lac.source}$	Lac.source (ABaCbcd) → Lac (ABaCbcd)
$V_{PC.L}$	Pyr (ABCcde) + CO2 (D) + H (f) + H (g) → 0.5*Oac (ABCfgD) + 0.5*Oac (DCBfgA) + H (c)
$V_{PCK.L}$	Oac (ABCabD) → PEP (ABCab) + CO2 (D)
$V_{CS.L}$	Oac (ABCcdD) + AcCoA (EFfgh) → Cit (DCcdBFfgEA) + H (h)
$V_{IDH.L}$	Cit (ABabCDcdEF) + H (e) → Akg (ABCeaDcdE) + H (b) + CO2 (F)
$V_{OGDH.L}$	Akg (ABCabDcdE) → SucCoA (BCabDcdE) + CO2 (A)
$V_{SDH.L}$	SucCoA (ABabCcdD) + H (e) + H (f) → 0.5*Oac (ABCefD) + 0.5*Oac (DCBefA) + H (a) + H
$V_{PCC.L}$	PropCoA (ABabCcde) + CO2 (D) → SucCoA (ACcdBabD) + H (e)
$V_{Bicarb.source}$	Bicarb.source (A) → CO2 (A)
$V_{Bicarb.sink}$	CO2 (A) → Bicarb.sink (A)
$V_{H.inf}$	H.inf (a) → H (a)
$V_{H.sink}$	H → H.sink
	^{13}C-Isotope Infusate Reactions
$V_{Lac.tracer}$	Lac.tracer (ABaCbcd) → Lac (ABaCbcd)
$V_{Prop.tracer}$	Prop.tracer (ABabCcde) → PropCoA (ABabCcde)

Table S1. Base reaction network for ^{2}H/^{13}C MFA. Related to Figures 2D, 2E and S1. The base model of liver metabolism tracks carbon (uppercase) and hydrogen (lowercase) atoms through the specified enzymatic reactions. Fluxes are regressed from plasma measurements of glucose MIDs using either $^{13}C_3$Lac/^{2}H or $^{13}C_3$Prop/^{2}H isotopes. Unenriched sources and sinks are denoted ".source" and ".sink", respectively. ^{2}H and ^{13}C isotopes are introduced into model reactions as ".tracer" sources. Compartments are denoted by ".P" for plasma and ".L" for liver. Liver is the default compartment if no compartment is designated for a metabolite. Simulations were performed post hoc from fluxes regressed to experimental labeling data. Unless otherwise noted here, reaction network and model assumptions have been described elsewhere (Hasenour et al., 2015)

Flux Reaction	Base Model $^{13}C_3$Lac/^{2}H	Base Model $^{13}C_3$Prop/^{2}H	Expanded Model $^{13}C_3$Lac/^{2}H	Expanded Model $^{13}C_3$Prop/^{2}H
$V_{CS.L}$	73 ± 6	100 ± 11	183 ± 28 [b]	195 ± 42
$V_{Enol.L}$	131 ± 16	131 ± 11	191 ± 20	189 ± 20
$V_{PYGL+GK.L}$	26 ± 4	29 ± 3	15 ± 7	14 ± 4
$V_{LDH.L}$	131 ± 16	106 ± 10	191 ± 20	164 ± 17
$V_{PC.L}$	141 ± 19	214 ± 22 [a]	363 ± 59 [b]	247 ± 69
$V_{PCK.L}$	141 ± 19	240 ± 22 [a]	363 ± 59 [b]	272 ± 74
$V_{PK+ME.L}$	9 ± 5	109 ± 13 [a]	172 ± 42 [b]	82 ± 63

Table S2. Comparison of selected flux estimates between base and expanded models of $^{13}C/^{2}H$ studies. Related to Figures 2 and 5, S1 and 7. [a] denotes fluxes that are significantly different between the $^{13}C_3$Lac/^{2}H and $^{13}C_3$Prop/^{2}H Base Models. [b] denotes fluxes that are significantly different between the $^{13}C_3$Lac/^{2}H Base and $^{13}C_3$Lac/^{2}H Expanded Models. Data presented as means (μmol/kg/min) ± SEM ($p \leq 0.05$, n=5-7)

Flux	Expanded Model Reaction Network (^{13}C transitions only)
	Liver Compartment: Glucose Synthesizing and Oxidative Metabolic Reactions
V_{EndoRa}	G6P (ABCDEF) → Glucose.P (ABCDEF)
$V_{Aldo.L}$	DHAP (ABC) + GAP (DEF) → G6P (CBADEF)
$V_{TPI.L}$	DHAP (ABC) ←→ GAP (ABC)
$V_{GAPDH.L}$	BPG (ABC) → GAP (ABC)
$V_{GK.L}$	Glycerol (ABC) → DHAP (ABC)
$V_{Enol.L}$	PEP (ABC) → BPG (ABC)
$V_{PK+ME.L}$	PEP (ABC) → Pyr (ABC)
$V_{LDH.L}$	Lac (ABC) ←→ Pyr (ABC)
$V_{Lac.source}$	Lac.source (ABC) → Lac (ABC)
$V_{ALT.L}$	Ala (ABC) ←→ Pyr (ABC)
$V_{PC.L}$	Pyr (ABC) + CO2 (D) → Oac (ABCD)
$V_{PCK.L}$	Oac (ABCD) → PEP (ABC) + CO2 (D)
$V_{PDH.L}$	Pyr (ABC) → AcCoA (BC) + CO2 (A)
$V_{\beta Oxid.L}$	Fat (AB) → AcCoA (AB)
$V_{CS.L}$	Oac (ABCD) + AcCoA (EF) → Cit (DCBFEA)
$V_{IDH.L}$	Cit (ABCDEF) ←→ Akg (ABCDE) + CO2 (F)
$V_{GDH.L}$	Glu (ABCDE) ←→ Akg (ABCDE)
$V_{Glu.source}$	Glu.source (ABCDE) → Glu (ABCDE)
$V_{OGDH.L}$	Akg (ABCDE) → SucCoA (BCDE) + CO2 (A)
$V_{SCS.L}$	SucCoA (ABCD) → Suc* (ABCD)
$V_{SDH.L}$	Suc* (ABCD) ←→ Fum* (ABCD)
$V_{FH.L}$	Fum* (ABCD) ←→ Mal (ABCD)
$V_{MDH.L}$	Mal (ABCD) ←→ Oac (ABCD)
$V_{Bicarb\ source}$	Bicarb.source (A) → CO2 (A)
$V_{Bicarb\ sink}$	CO2 (A) → Bicarb.sink (A)
	^{13}C-Isotope Infusate Reactions
$V_{Lac.tracer}$	Lac.inf (ABC) → Lac (ABC)
$V_{Lac.inf}$	Lac.inf (ABC) → Lac.P (ABC)

Table S3. Expanded reaction network for ^{13}C MFA. Related to Figures 4, S4 and S6. (Table and caption continues to next page)

Extrahepatic Compartment: Glycolytic, and Cori Cycle Reactions	
$V_{HK.E}$	Glucose.P (ABCDEF) → G6P.E (ABCDEF)
$V_{PYGM.E}$	Glycogen.E (ABCDEF) → G6P.E (ABCDEF)
$V_{Aldo.E}$	G6P.E (ABCDEF) → GAP.E (CBA) + DHAP.E (DEF)
$V_{TPI.E}$	GAP.E (ABC) ←→ DHAP.E (ABC)
$V_{GAPDH.E}$	GAP.E (ABC) → BPG.E (ABC)
$V_{Enol.E}$	BPG.E (ABC) → PEP.E (ABC)
$V_{PK.E}$	PEP.E (ABC) → Pyr.E (ABC)
$V_{PyrOxid.E}$	Pyr.E (ABC) → CO2 (A) + CO2 (B) + CO2 (C)
$V_{LDH.E}$	Pyr.E (ABC) ←→ Lac.P (ABC)
$V_{LacTransport}$	Lac.P (ABC) → Lac (ABC)

Table S3 (Continued). Expanded reaction network for ^{13}C MFA. Related to Figures 4, S4 and S6. Expanded model of liver metabolism for tracking only carbon atoms through the specified enzymatic reactions. Fluxes are regressed from liver and plasma measurements for mice infused with $^{13}C_3$Lac. Unenriched sources and sinks are denoted ".source" and ".sink", respectively. Infused ^{13}C isotopes are introduced into model reactions as ".tracer" sources in liver-only models or ".inf" sources for two-compartment models. (Note that these two types of tracer input fluxes are not expected to be equivalent in the case of $^{13}C_3$Lac administration, since $V_{Lac.tracer}$ represents liver-specific uptake of the tracer while $V_{Lac.inf}$ represents infusion of tracer into the plasma compartment.) Compartments are denoted by ".P" for plasma, ".E" for extrahepatic, and ".L" for liver. Liver is the default compartment if no compartment is designated for a metabolite. The two-compartment model includes reactions for the liver, ^{13}C-bicarbonate recycling, and Cori cycle reactions. *denotes that the carbons of succinate and fumarate are symmetric

Flux	Expanded Model Reaction Network ($^{2}H/^{13}C$ transitions)
	Expanded Liver Compartment: Glucose Synthesizing and Oxidative Metabolic Reactions
$V_{Glc.Inf}$	Glucose.inf (AaBbCcDdEeFfg) → Glucose.P (AaBbCcDdEeFfg)
V_{EndoRa}	G6P (AaBbCcDdEeFfg) → Glucose.P (AaBbCcDdEeFfg)
$V_{PYGL.L}$	Glycogen (AaBbCcDdEeFfg) + H (h) → G6P (AaBhCcDdEeFfg) + H (b)
$V_{Aldo.L}$	DHAP (AabBCcd) + GAP (DeEfFgh) + H (i) → G6P (CdBiAaDeEfFgh) + H (b) + H (c)
$V_{TPI.L}$	DHAP (AabBCcd) + H (e) ←→ GAP (AbBeCcd) + H (a)
$V_{GAPDH.L}$	BPG (ABbCcd) + H (a) → GAP (AaBbCcd)
$V_{GK.L}$	Glycerol (AabBeCcd) → DHAP (AabBCcd) + H (e)
$V_{Enol.L}$	PEP (ABCcd) + H (b) → BPG (ABbCcd)
$V_{PK+ME.L}$	PEP (ABCab) + H (c) → Pyr (ABCabc)
$V_{LDH.L}$	Lac (ABbCcde) ←→ Pyr (ABCcde) + H (b)
$V_{Lac.source}$	Lac.source (ABbCcde) → Lac (ABbCcde)
$V_{ALT.L}$	Ala (ABbCcde) + H (f) ←→ Pyr (ABCcdf) + H (b) + H (e)
$V_{PC.L}$	Pyr (ABCcde) + CO2 (D) → Oac (ABCcdD) + H (e)
$V_{PCK.L}$	Oac (ABCabD) → PEP (ABCab) + CO2 (D)
$V_{CS.L}$	Oac (ABCcdD) + AcCoA (EFfgh) → Cit (DCcdBFfgEA) + H (h)
$V_{IDH.L}$	Cit (ABabCDcdEF) + H (e) ←→ Akg (ABCeaDcdE) + H (b) + CO2 (F)
$V_{GDH.L}$	Glu (ABeCabDcdE) ←→ Akg (ABCabDcdE) + H (e)
$V_{OGDH.L}$	Akg (ABCabDcdE) → SucCoA (BCabDcdE) + CO2 (A)
$V_{SCS.L}$	SucCoA (ABabCcdD) → Suc* (ABabCcdD)
$V_{PCC.L}$	PropCoA (ABabCcde) + CO2 (D) → SucCoA (ACcdBabD) + H (e)
$V_{SDH.L}$	Suc* (ABabCcdD) ←→ Fum* (ABaCdD) + H (b) + H (c)
$V_{FH.L}$	Fum* (ABaCbD) + H (c) ←→ Mal (ABaCcbD)
$V_{MDH.L}$	Mal (ABaCbcD) ←→ Oac (ABCbcD) + H (a)
$V_{Bicarb.source}$	Bicarb.source (A) → CO2 (A)
$V_{Bicarb.sink}$	CO2 (A) → Bicarb.sink (A)
$V_{H.inf}$	H.inf (a) → H (a)
$V_{H.sink}$	H → H.sink

Table S4. Expanded reaction network for $^{2}H/^{13}C$ MFA. Related to Figures 5 and S7. (Table and caption continues to next page)

	^{13}C-Isotope Infusate Reactions
$V_{Lac.inf}$	Lac.inf (ABbCcde) → Lac.P (ABbCcde)
$V_{Prop.inf}$	Prop.inf (ABabCcde) → PropCoA (ABabCcde)

	Expanded Extrahepatic Compartment: Glycolytic, and Cori Cycle Reactions
$V_{HK.E}$	Glucose.P (AaBbCcDdEeFfg) → G6P.E (AaBbCcDdEeFfg)
$V_{PYGM.E}$	Glycogen.E (AaBbCcDdEeFfg) + H (h) → G6P.E (AaBhCcDdEeFfg) + H (b)
$V_{Aldo.E}$	G6P.E (CdBiAaDeEfFgh) + H (b) + H (c) → DHAP.E (AabBCcd) + GAP.E (DeEfFgh) + H (i)
$V_{TPI.E}$	DHAP.E (AabBCcd) + H (e) ←→ GAP.E (AbBeCcd) + H (a)
$V_{GAPDH.E}$	GAP.E (AaBbCcd) → BPG.E (ABbCcd) + H (a)
$V_{Enol.E}$	BPG.E (ABbCcd) → PEP.E (ABCcd) + H (b)
$V_{PK.E}$	PEP.E (ABCab) + H (c) → Pyr.E (ABCabc)
$V_{ALT.E}$	Ala.E (ABbCcde) + H (f) ←→ Pyr.E (ABCcdf) + H (b) + H (e)
$V_{PyrOxid.E}$	Pyr.E (ABCcde) → H (c) + H (d) + H (e) + CO2 (A) + CO2 (B) + CO2 (C)
$V_{LDH.E}$	Pyr.E (ABCcde) + H (b) ←→ Lac.P (ABbCcde)
$V_{LacTransport}$	Lac.P (ABbCcde) → Lac (ABbCcde)

Table S4 (Continued). Expanded reaction network for ^{2}H/^{13}C MFA. Related to Figures 5 and S7. Expanded model of liver metabolism for tracking both carbon (uppercase) and hydrogen (lowercase) atoms through the specified enzymatic reactions. Fluxes are regressed from liver and plasma measurements using either $^{13}C_3$Lac/^{2}H or $^{13}C_3$Prop/^{2}H isotopes. See Tables S1 and S3 for nomenclature

Metabolite	m/z	Formula	Carbons
Alanine	260	$C_{11}H_{26}O_2NSi_2$	1 2 3
Alanine	232	$C_{10}H_{26}ONSi_2$	2 3
Aspartate	390	$C_{17}H_{40}O_3NSi_3$	2 3 4
Aspartate	418	$C_{18}H_{40}O_4NSi_3$	1 2 3 4
α-Ketoglutarate	346	$C_{14}H_{28}O_5NSi_2$	1 2 3 4 5
Glutamate	432	$C_{19}H_{42}O_4NSi_3$	1 2 3 4 5
Glutamate	330	$C_{16}H_{36}O_2NSi_2$	2 3 4 5
Glucose	370	$C_{17}H_{24}O_8N$	1 2 3 4 5
Glucose	301	$C_{14}H_{21}O_7$	1 2 3 4 5 6
Glucose	284	$C_{13}H_{18}O_6N$	1 2 3 4
Glucose	259	$C_{12}H_{19}O_6$	4 5 6
Glucose	173	$C_8H_{13}O_4$	5 6
Glucose	145	$C_6H_{11}O_3N$	1 2
Lactate	261	$C_{11}H_{25}O_3Si_2$	1 2 3
Lactate	233	$C_{10}H_{25}O_2Si_2$	2 3
Urea	231	$C_9H_{23}N_2OSi_2$	1

Table S5. Measured GC-MS fragment ions. Related to all Figures.